AN EFFICIENT ATTENUATION COMPENSATION METHOD USING THE SYNCHROSQUEEZING TRANSFORM

YANG YANG[1,3], JINGHUAI GAO [2,3], GUOWEI ZHANG[3] and QIAN WANG[3]

[1] *School of Electronic and Information Engineering, Xi'an Jiaotong University, 28 Xianning West Road, Xi'an 710049, P.R. China. yang.yang.891015@stu.xjtu.edu.cn*
[2] *School of Electronic and Information Engineering, Xi'an Jiaotong University, 28 Xianning West Road, Xi'an 710049, P.R. China. jhgao@mail.xjtu.edu.cn*
[3] *National Engineering Laboratory for offshore oil Exploration, Xi'an Jiaotong University, 28 Xianning West Road, Xi'an 710049, P.R. China.*

(Received August 4, 2017; revised version accepted September 24, 2018)

ABSTRACT

Yang, Y., Gao, J.H., Zhang, G.W. and Wang, Q., 2018. An efficient attenuation compensation method using the synchrosqueezing transform. *Journal of Seismic Exploration*, 27: 577-591.

Attenuation of seismic waves, which decreases the amplitude and distorts the phase, also usually results in low resolution of seismic data. In this study, inverse Q filtering is introduced to compensate the attenuation of seismic waves using the synchrosqueezing transform (SST), which condenses the spectrum energy along the frequency axis and provides highly localized time-frequency representations. To perform a stable inverse Q filtering, a denoising filtering and reliable Q values are needed. At first, a spare SST-domain filtering is utilized to remove the random noise based on a low-rank and spare decomposition-based method. Then, a reliable Q-factor estimation method using the peak frequency shift method in SST domain is applied in the implementation of inverse Q filtering scheme. At last, we reformulate amplitude correction as an inverse problem with a l_2-norm regularization term in the SST domain to prevent the noise bursting because of the inherently unstable process of amplitude correction. Therefore, we propose a complete three-stage work flow to denoise, estimate Q factor and compensate attenuation using the SST. Tests with synthetic examples and real data demonstrate the robustness and effectiveness of this proposed method.

KEY WORDS: synchrosqueezing transform (SST), denoise, Q estimation, inverse Q filtering.

0963-0651/18/$5.00

INTRODUCTION

Attenuation of seismic waves, defined by the quality factor Q, always brings some undesirable effects in seismic data processing. It attenuates the high-frequency components and distorts the phase of the wavelets, leading to great degradation of the resolution of seismic data. Corrections for these viscoelastic effects are necessary to enhance the resolution and facilitate the seismic data interpretation (van der Baan, 2012; Yilmaz, 2001). A complete work flow to correct attenuation of seismic data should include high signal-to-noise ratio (SNR) seismic data ((Boashash and Meshah, 2004; Cheng et al., 2015; Yang et al., 2013; Trickett 2008), reliable Q values (Tonn, 1991; Reine, 2012; Quan and Harris, 1997; Zhang and Ulrych, 2002; Wang, 2004; Gao et al.,2011; Tary, 2016; Lupinacci et al., 2016; Wang et al., 2014) and a stable inverse Q filtering (Wang, 2002, 2006; Braga and Moraes, 2013; Lupinacci et al., 2016) which is always an unstable process of amplitude correction.

To obtain the high SNR of seismic data, a denoising filtering is first needed. Generally, the random noise, which is not correlated from trace to trace, can be separated from the seismic data to improve the SNR of seismic data (Boashash and Meshah, 2004; Cheng et al., 2015). According to the geometric distribution structures of the seismic data and the random noise, the seismic data can be recovered from the low-rank matrix (Yang et al., 2013; Trickett, 2008) in low-rank and spare decomposition methods, such as robust principal component analysis (RPCA; Candès and Plan, 2010; Chen and Sacchi, 2015) and go-decomposition (GoDec; Zhou and Tao, 2011) method. Nazari Siahsar (2016) proposed an efficient low-rank and spare decomposition-based denoising filtering to improve the SNR of the seismic data, which combines Semi-Soft go-decomposition-based method (Semi-soft GoDec) and the SST transform. Thus, we use this filtering to removal the random noise as the preparation operation in our proposed work flow.

To achieve accurate Q factors from seismic data is another significant issue. Various methods have been proposed for Q estimation in the frequency domain, such as the spectral ratio method (Tonn, 1991; Reine, 2012) and the frequency shift method (Quan and Harris, 1997; Zhang and Ulrych, 2002). The Q factor can also be estimated in the time-frequency domain (Wang, 2004; Tary, 2016; Lupinacci et al., 2016; Wang et al., 2014). Tary (2016) developed a method to obtain a reliable and robust estimation of quality factor by combining the peak frequency shift method with the SST. Therefore, we can incorporate this method into the work flow to estimate Q values as the vital input of inverse Q filtering.

At last, many researches have been published to develop a stable and efficient inverse Q filtering scheme. The phase compensation method (Hargreaves, 2012) used a constant Q value to correct phase dispersion without considering amplitude compensation. The amplitude compensation is an inherently unstable process since the amplitude compensation operator is an increasing exponential function of time and frequency. The instability problem has been partially solved by incorporating a stabilization factor

(Wang, 2002, 2006), which is equal to solving an inverse problem with a l_2-norm regularization term (Braga and Moraes, 2013; Lupinacci et al., 2016). Typically, inverse Q filtering can be implemented in the time-frequency (scale) domain. Wang (2006) proposed an inverse Q filtering scheme using Gabor transforms. Braga and Moaes (2013) introduced the continuous wavelet transform (CWT) to compensate the amplitude loss. However, the Gabor transform and CWT produce energy smearing along the frequency or scale axis. The recently developed synchrosqueezing transform (Daubechies et al., 2009, 2011), which reduces the time-frequency spectral smearing, provides highly localized and accurate time-frequency representations for non-stationary signals. Consequently, the SST can be also introduced in the implementation of inverse Q filtering.

In this work, we propose a three-stage work flow to remove the random noise, estimate the Q factor and correct the attenuation using the synchrosqueezing transform. First, we describe the theory of SST to obtain the highly localized time-frequency maps. Second, we introduce a low-rank and spare decomposition-based denoising filtering using the SST transform as the preparation of seismic data. Third, we discuss the peak frequency shift method for Q estimation trace by trace. Moreover, the l_2-norm regularization method to stabilize the inverse Q filtering scheme is proposed. Finally, synthetic and field data examples are provided to demonstrate the validity of the proposed method.

METHOD

The Synchrosqueezing Transform (SST)

Compared with empirical mode decomposition (EMD), SST has a firm mathematical theory foundation based on the CWT (Thakur et al., 2013; Daubechies et al., 2009, 2011). The Synchrosqueezing Transform provides highly localized time-frequency representation based on reassignment techniques.

The SST technique assumes that a muti-component signal $s(t)$ consists of harmonic components and additive noise $n(t)$, given by

$$s(t) = \sum_{n=1}^{N} A_n(t)\cos(\phi_n(t)) + n(t) \quad , \tag{1}$$

where $A_n(t)$ is the instantaneous amplitude, $\phi_n(t)$ is the instantaneous phase of the n-th component, respectively. The CWT coefficient of signal is $s(t)$ defined by

$$W_s(a,b) = \frac{1}{\sqrt{a}}\int s(t)\psi^*(\frac{t-b}{a})dt \quad , \tag{2}$$

where ψ^* is the complex conjugate of the mother wavelet ψ, a and b are the scale and time shift variables, respectively. Due to the uncertain principle, the wavelet coefficients $W_s(a,b)$ will spread out around scale axis in the time-scale plane. To reduce this effect, a reassignment technique is performed according to the instantaneous frequency information, which is given by

$$f_s(a,b) = \frac{-i}{2\pi W_s(a,b)} \frac{\partial W_s(a,b)}{\partial b}, \ for\ W_s(a,b) \neq 0 \quad . \tag{3}$$

Then, the SST is computed based on the instantaneous frequency $f_s(a,b)$, defined by

$$T_s(f,b) = \int_{\{a:W_s(a,b)\neq 0\}} W_s(a,b) a^{-3/2} \delta(f - f_s(a,b)) \quad . \tag{4}$$

As a result, the $W_s(a,b)$ in the time-scale plane is mapped to $T_s(f,b)$ in the time-frequency plane. Fig. 1 shows the time-frequency spectrum of test signals $s(t) = s_1(t) + s_2(t)$, which defined by $s_1(t) = \sin(2(150\pi t + 40(\sin(2\pi t))))$ and $s_2(t) = \sin(2(60\pi t + 20(\sin(2\pi t))))$. The SST (Fig. 1(c)) can achieve higher time-frequency resolution compared with the CWT (Fig. 1(b)). The synchrosqueezing transform can be also applied to seismic time-frequency analysis (Wang et al., 2014; Herrera et al., 2014), shown in Fig. 2. Compared the CWT (Fig. 2(b)) and SST spectrum (Fig. 2(c)), the SST can provide highly localized time-frequency representation. In addition, the SST is also introduced to noise removal (Nazari Siahsar et al., 2016) and attenuation estimation (Tary et al., 2016).

SST-domain filtering

In this section, an efficient denoising method, based on Semi-Soft go-decompostion (Zhou and Tao, 2011), is introduced. This method transforms the seismic data into a spare time-frequency space using SST transform. In this time-frequency space, the seismic signals and random noise will be separated (Nazari Siahsar et al., 2016). Now, we display the Semi-soft Godec algorithm to decompose the SST spectrum $\mathbf{T}$ of seismic data into a low-rank $\mathbf{L}$ and a sparse part $\mathbf{S}$, defined by

$$\mathbf{T} = \mathbf{L} + \mathbf{S} + \mathbf{E} \quad s.t.\ \ rank(\mathbf{L}) \leq p \,\&\, card(\mathbf{S}) \leq q \quad , \tag{5}$$

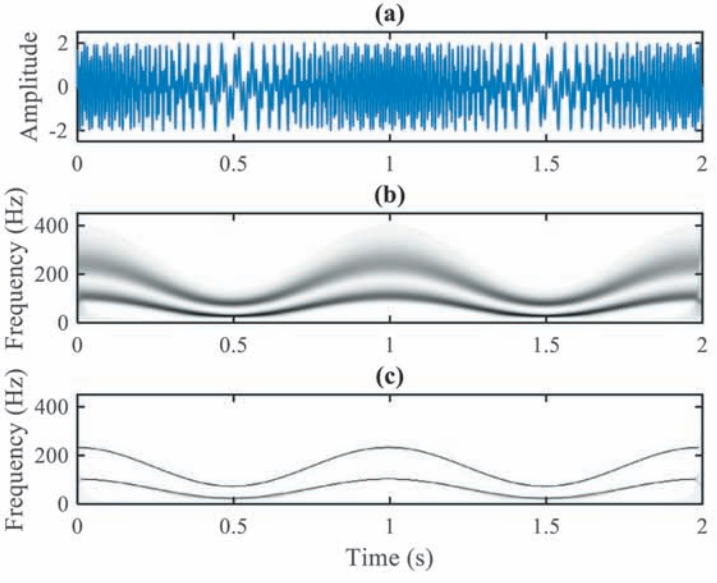

Fig. 1. The time-frequency spectrum of CWT and SST for test signals. (a) The test signals. (b) The CWT spectrum of test signals. (c) The SST spectrum of test signals.

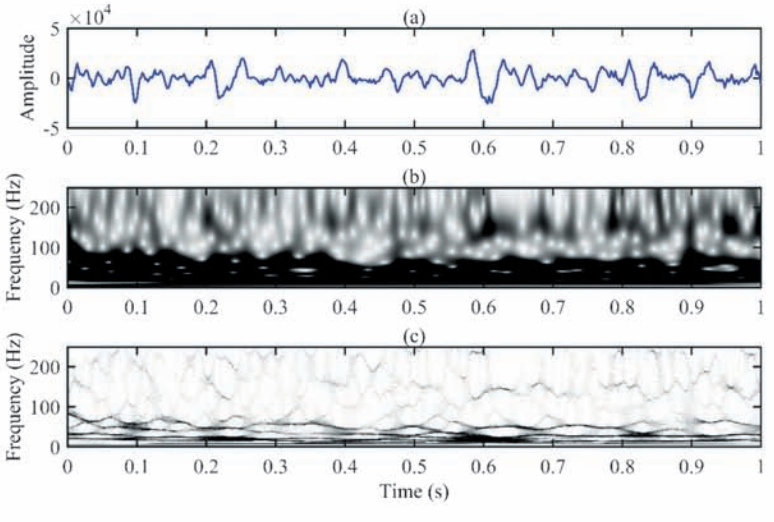

Fig. 2. The time-frequency spectrum of CWT and SST for a real seismic data. (a) A real seismic data. (b) The CWT spectrum of the real seismic data. (c) The SST spectrum of the real seismic data.

where $\mathbf{E}$ is the decomposition error. p is the max rank of $\mathbf{L}$. q is the max number of non-zero elements of $\mathbf{S}$, which is also defined by the l_0-norm. In order to decrease the time cost and make the problem easy operation, Zhou and Tao introduce the minimization Frobenius regularization to replace the 'hard' constraint of eq. (5), given by:

$$\min_{\mathbf{L},\mathbf{S}} \|\mathbf{T}-\mathbf{L}-\mathbf{S}\|_F^2 + \eta\|\mathbf{S}\|_1 \ \ s.t.\ rank(\mathbf{L}) \le p \quad , \tag{6}$$

where the l_1-norm, which is the tightest convex relation of the l_0-norm, adds the sparse constraint to the main function. η is the soft thresholding to balance the sparse constraint and low-rank constraint.

In this iterative Semi-Soft GoDec algorithm, the low-rank components are estimated by bilateral random projection (BRP) instead of unilateral random projection, which is used in randomized SVD method. The low-rank part $\mathbf{L}^t$, which is regarded as a fast rank-p approximation of an $m \times n$ matrix $\mathbf{T}$ at iterative t, is estimated by two random projections $\mathbf{Y}_1 = \mathbf{T}\mathbf{A}_1$ and $\mathbf{Y}_2 = \mathbf{T}^{\mathrm{T}}\mathbf{A}_2$ from eq. (7):

$$\mathbf{L}^t = \mathbf{Y}_1(\mathbf{A}_2^{\mathrm{T}}\mathbf{Y}_1)^{-1}\mathbf{Y}_2^{\mathrm{T}} \quad , \tag{7}$$

where $\mathbf{A}_1 \in \mathbf{R}^{n\times p}$ and $\mathbf{A}_2 \in \mathbf{R}^{m\times p}$ are random matrices. The spare component $\mathbf{S}^t$ of $\mathbf{T}$ is updated by soft-thresholding of $\mathbf{T}-\mathbf{L}^t$,

$$\mathbf{S}^t = F_\eta(\mathbf{T}-\mathbf{L}^t),\ F_\eta(x) = sign(x)\max(|x|-\eta, 0) \quad . \tag{8}$$

Fig. 3 shows a scheme of SST-domain filtering on a synthetic seismic data (Fig. 3(a)), which contains three 35 Hz Richer wavelets added with Gauss white noise (SNR = 0 dB). The time duration is 1 s and time sampling interval is 1 ms. First, we transform the seismic data into the spare time-frequency domain using the SST transform (Fig. 3(b)). The normalization singular values of the SST spectrum are indicated in Fig. 4. As can be seen from Fig. 4, the SST spectrum of seismic data can be decomposed into low-rank (Fig. 3(d)) and spare (Figs. 3(e) and 3(f)) part according to the Semi-Godec method. Therefore, the denoised SST spectrum is approximately recovered from a small number of the largest singular values, shown in Fig. 3(c). Compared with the noise-free seismic data (Fig. 3(g)), the recovered seismic data (Fig. 3(c)) based on SST-domain filtering is noiseless and similar to the noise-free seismic data (Fig. 3(g)). In this example, the parameter of rank and η is 6 and 0.00001, respectively.

Q-factor estimation

In this section, we give a brief description of the peak frequency shift method to estimate Q-factor (Zhang and Ulrych, 2002). Fig. 5(a) shows the Ricker wavelets considering only amplitude changes with 35 Hz propagated through an attenuating and dispersive medium with constant Q factor of 60. As time increases, the peak frequency of these three wavelets translates toward lower frequency and the frequency width becomes wider, which is illustrated in Fig. 5(b). According to the attenuation model (Kolsky,

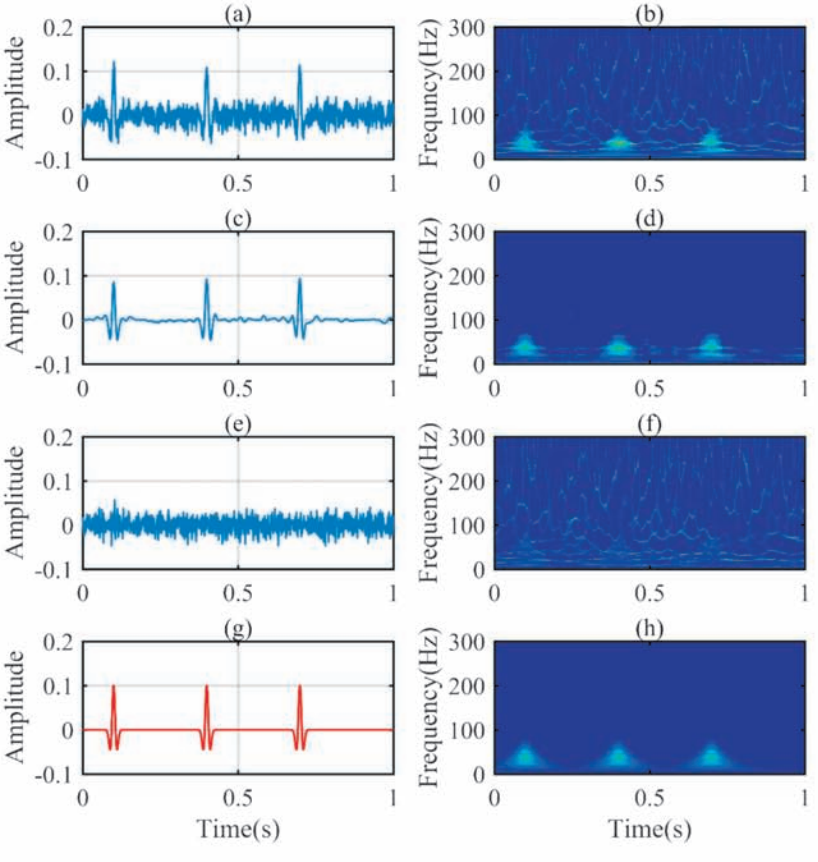

Fig. 3. A scheme of SST- domain denoising on synthetic data with SNR = 0 dB. (a) The input synthetic seismic data including three 35 Hz Richer wavelet with Gauss white noise (SNR = 0 dB). (b) The SST spectrum of the input synthetic seismic data. (c) The recovered wavelets from the SST-domain filtering. (d) The SST spectrum of the recovered wavelets. (e) and (f) are estimated random noise in time domain and time-frequency domain, respectively. (g) The noise-free synthetic seismic data. (h) The SST spectrum of (g).

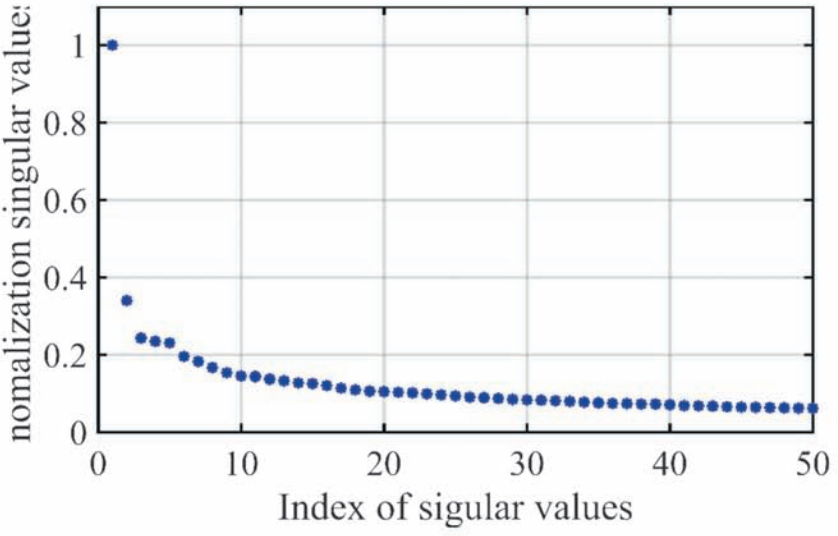

Fig. 4. Normalization Singular spectrum.

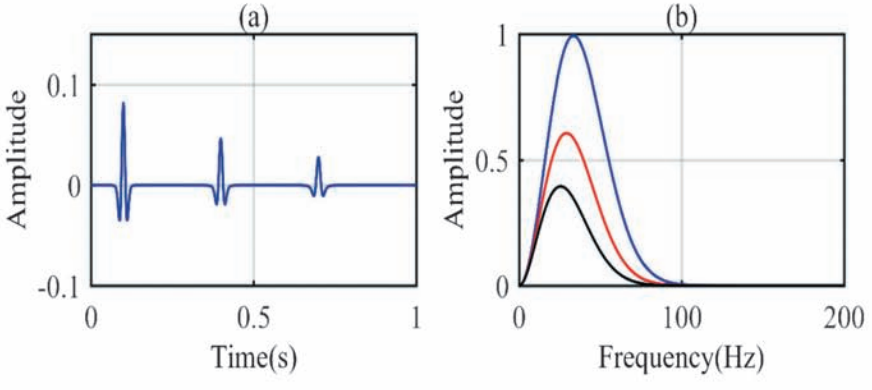

Fig. 5. Attenuation of the seismic data reduces the peak frequency of Fourier spectrum. (a) The Ricker wavelets considering only amplitude changes with 35 Hz propagated through an attenuating and dispersive medium with constant factor of 60. (b) The Fourier spectrum of the three wavelets in (a). The black line is the Fourier spectrum at 0.7 s. The red one is at 0.4 s. The blue one is at 0.1 s.

1956; Wang, 2009), the received spectrum $A_R(t,f)$ of a seismic data is most significantly correlated with the source spectrum $A_s(f)$ (Aki and Richards, 2002), defined by:

$$A_R(t,f) = GA_s(f)\exp(-\frac{\pi ft}{Q}) \quad , \tag{9}$$

where G, independent of frequency, represents the geometric spreading factor, t is travel time and f is frequency. In many situations, the amplitude spectrum of source can be approximated by a Ricker wavelet spectrum (Ricker, 1953):

$$A_s(f) = \frac{2}{\sqrt{\pi}} \frac{f^2}{f_0^3} \exp(-\frac{f^2}{f_0^2}) \quad , \tag{10}$$

where f_0 is the peak frequency of the source spectrum. From equations (9) and (10), the peak frequency f_p of the received spectrum can be obtained by setting the derivation of spectrum $A_R(t,f)$ with respect to frequency to zero:

$$f_p = f_0^2 \left[\sqrt{\left(\frac{\pi t}{4Q}\right)^2 + \left(\frac{1}{f_0}\right)^2} - \frac{\pi t}{4Q} \right] \quad . \tag{11}$$

Then the Q-factor can be estimated by the variation of peak frequency:

$$Q = \frac{\pi t f_p f_0^2}{2\left(f_0^2 - f_p^2\right)} \quad . \tag{12}$$

In practice, the peak frequency f_0 of source wavelet is always unknown, we can calculate the f_0 with the peak frequency f_{p1} and f_{p2} at time t_1 and t_2:

$$f_0 = \sqrt{\frac{f_{p1} f_{p2} (t_2 f_{p1} - t_1 f_{p2})}{t_2 f_{p2} - t_1 f_{p1}}} \quad . \tag{13}$$

Due to the peak frequency sensitivity to the noise and systematic biases, we first use amplitude smoothing method (Zhou et al., 2014; Rosa, 1991) to smooth the spectrum, which is given by:

$$T(f) = |f|^K \exp(H(f)) \quad , \tag{14}$$

where K is a positive constant and $H(f)$ is a polynomial of f. Then, the center frequency is introduced instead to estimate quality factor Q, which is more stable and given by (Tary, 2017)

$$f_c = \frac{\int_0^\infty f A_R(f) df}{\int_0^\infty A_R(f) df} \quad , \tag{15}$$

Inverse *Q* filtering

The main concern of attenuation compensation is the stability. Braga and Moraes (2013) introduced l_2-norm regularization method to stabilize the inverse Q filtering scheme in the wavelet transform domain. Similarly, we also reformulate the amplitude compensation as an inverse problem with a l_2-norm regularization term in the SST domain.

In the SST domain, without considering the phase changes, the compensation process can be given by

$$T_{S_0}(t,f) = T_S(t,f)\exp(\frac{\pi ft}{Q}) \quad , \tag{16}$$

where $T_{S_0}(t,f)$ and $T_S(t,f)$ are the time-frequency representations of the original unaffected signal $s_0(t)$ and attenuated signal $s(t)$, respectively. The compensation output $s_0(t)$ can be obtained through the inverse SST transform (Daubechies et al., 2011):

$$s_0(t) = C_\psi \Re e\left[\int_0^\infty T_{s_0}(t,f)df\right] \quad , \tag{17}$$

where C_ψ is a constant depending on the mother wavelet ψ. Note that the amplitude compensation operator $\exp(\pi ft/Q)$ is an increasing exponential function of time and frequency. Direct amplitude compensation using eq. (16) will cause instability and generate undesirable artifacts.

For stabilization, it is reformulated as an inverse problem, where a regularized solution can be achieved by minimizing the cost function,

$$\phi(\mathbf{T}_{\mathbf{s_0}}, \lambda) = \left\|\mathbf{T_s} - \mathbf{G}\mathbf{T}_{\mathbf{s_0}}\right\|_2^2 + \lambda\left\|\mathbf{T}_{\mathbf{s_0}}\right\|_2^2 \quad , \tag{18}$$

as given by

$$\mathbf{T}_{\mathbf{s_0}} = \left(\mathbf{G}^{\mathrm{T}}\mathbf{G} + \lambda\mathbf{I}\right)^{-1} G^T\mathbf{T_s} \quad , \tag{19}$$

where $\mathbf{G}$ is a $N \times L$ diagonal matrix of the forward attenuation operator, which is defined $\mathbf{G} = diag(vec(g_{ij}))$. The elements of $\mathbf{G}$ are $g_{ij} = -\pi f_j t_i / Q$ for $i = 1,2...N$ and $j = 1,2...L$, where N and L represent the number of time samples and frequency samples, respectively. $\mathbf{T}_{\mathbf{s_0}}$ and $\mathbf{T_s}$ are vectorized versions of $T_{S_0}(t,f)$ and $T_S(t,f)$, whose elements are taken column-wise from the corresponding matrices. The regularization parameter λ is particularly crucial to balance the amplitude of correction

seismic data and the noise. Smaller values of λ cannot correct the attenuation signal without larger noise, but larger values of λ bring much more noise. In this paper, the value of λ is given as 0.001 for most situations (Braga and Moraes, 2013).

Proposed work flow

In this paper, we present a complete three-stage work flow to compensate the attenuation of seismic data. The complete work flow is as follows:

1) Transform seismic data into the time-frequency domain trace by trace using the SST transform;
2) Decompose the SST spectrum into low-rank and spare part by solving the eq. (6) using semi-soft Godec method, then use the low-rank p part as the denoised SST spectrum;
3) Estimate Q factor using the peak frequency shift method using eq. (12) in the SST domain;
4) Set the Q values and the denoised SST spectrum as the input of the proposed inverse Q filtering, and apply eq. (19) to compensate the amplitude in SST domain;
5) Use the inverse SST transform to the obtained result of inverse Q filtering.

SYNTHETIC AND REAL DATA EXAMPLES

Synthetic and real seismic data are used to verify the efficiency of the proposed work flow for attenuation correction. First, a noise-free synthetic trace, shown in Fig. 6(a), contains a Ricker wavelet considering only amplitude changes with 35 Hz propagated through an attenuating and dispersive medium with constant factor of 60. The time duration is 1s and time sampling interval is 1 ms. The factor value of this noise-free synthetic data, estimated by eq. (12), is 61.96. Fig. 6(b) shows the enhanced trace by inverse Q filter using SST. It is clearly seen that the recovered wavelet and amplitude spectrum is similar to the original wavelet without amplitude attenuation (the red line in Fig. 3(g)).

To confirm the robustness and the effectiveness of the proposed method, Gaussian random noise is added with the input trace (SNR = 0 dB), shown in Fig. 7(a). At first, the SST-domain filtering is operated on the noisy wavelet. The parameter values of rank p and η are 10 and 0.00003, respectively. Compared with the noisy wavelet, a largest number of noises are removed and the SNR of synthetic seismic wavelet is improved, shown in Fig. 7(c). And then, the proposed inverse Q filter in SST domain is used to compensate the de-noised wavelet with the estimated attenuation factor 69.67. Note that the recovery amplitude in Fig. 7(e) is similar to the noise-free wavelet (Fig. 3(g)) and our proposed operation prevents noise from bursting up.

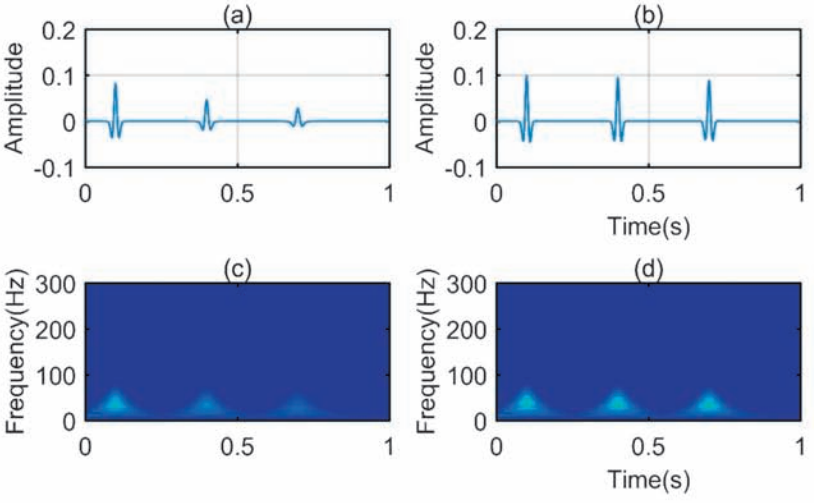

Fig. 6. The proposed attenuation correction method applied on a noise-free synthetic seismic data. (a) The input of noise-free seismic wavelet with attenuation factor 60. (b) The output of attenuation compensation for noise-free wavelet with estimated attenuation factor 61.96. (c) and (d) are amplitude spectrum in the SST domain.

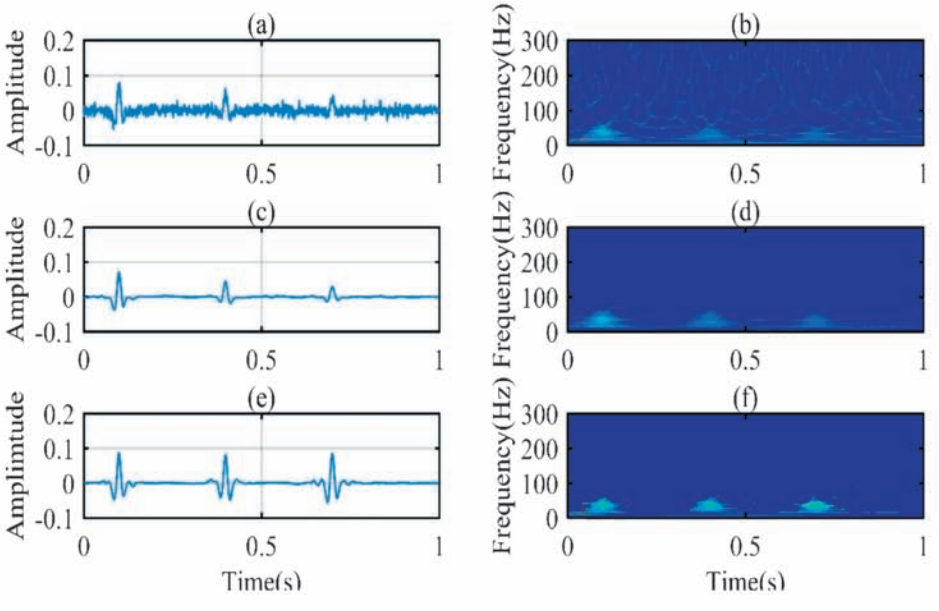

Fig. 7. The proposed attenuation correction method applied on a noisy synthetic seismic data. (a) The input of noisy seismic wavelet with attenuation factor 60 and SNR = 0 dB. (c) The denoised wavelet using SST-domain filter. (b) and (d) are the SST spectrum of the noisy wavelet and the denoised wavelet, respectively. (e) The output of attenuation compensation for denoised wavelet with estimated attenuation factor 69.67. (f) The SST amplitude spectrum of attenuation compensated wavelet.

Finally, we apply the attenuation correction flow to a field post-stack data, shown in Fig. 8, which contains 251 traces and 502 sample points. The time sampling interval is 1ms. The rank p and η parameter is 10 and 0.00005, respectively. Phase dispersion has been corrected in the previous processing. We only consider the amplitude compensation. The recovery seismic data are illustrated in Fig. 8(c). The vertical resolution is improved, especially in the deep part, as marked by the black rectangles. The time-frequency amplitude spectrum of 150th trace is shown in Figs. 8(b) and 8(d), which describes a broader time-frequency distribution of energy. Fig. 9 shows the average Fourier spectrum comparison of the 100th, 150th and 200th seismic traces of Fig. 8. Compared with the original Fourier spectrum (the red line in Fig. 9), the recovered Fourier spectrum (the blue line in Fig. 9) is much higher, especially in high frequency.

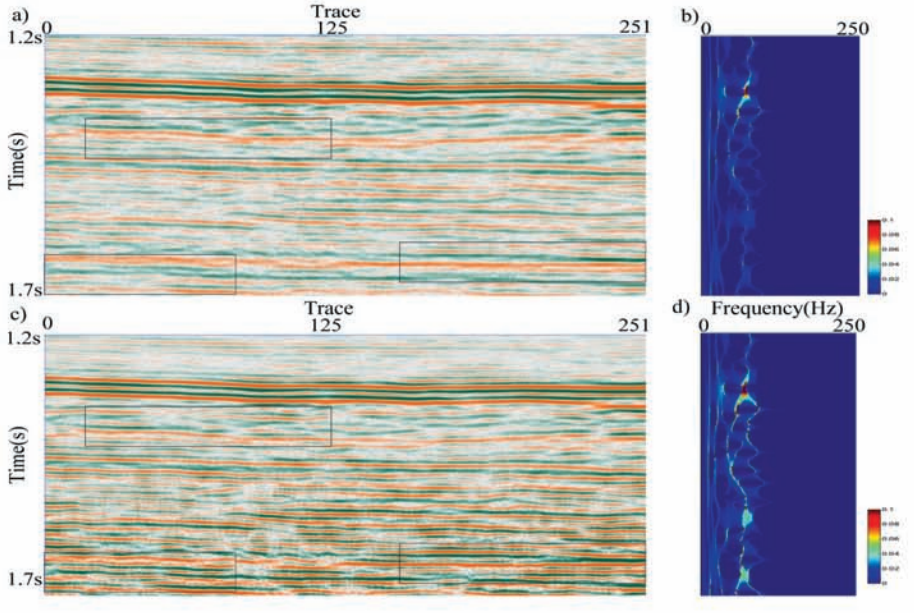

Fig. 8. The proposed attenuation correction method applied on a real seismic data. (a) The input real seismic data. (c) The recovered real seismic data from our proposed work flow. (b) and (d) are the SST spectrum of the input and recovered real seismic data of 150th seismic trace, respectively.

CONCLUSIONS

We have proposed a complete work flow to remove the rand noise, estimate the Q factor and compensate attenuation using the SST. To obtain a high SNR seismic data, the semi-soft GoDec-based filtering combined with SST is applied. Then, the peak frequency shift method in SST domain is

illustrated to receive a reliable quality factor as an input parameter for amplitude compensation. The attenuation correction is also implemented in the SST domain. Since it is an inherently unstable process, we reformulate it as a regularized inverse problem. Numerical examples on synthetic and field data demonstrate that the proposed flow can restore the high-frequency components, and thus enhance the resolution of seismic data.

ACKNOWLEDGEMENTS

We greatly appreciate the Major Programs of National Natural Science Foundation of China under grant No.41390454 for their financial support. We also greatly appreciate the National Science and Technology Major Project of China under grant No.2016ZX05024-001-007 and No.2017ZX05069 for their financial support.

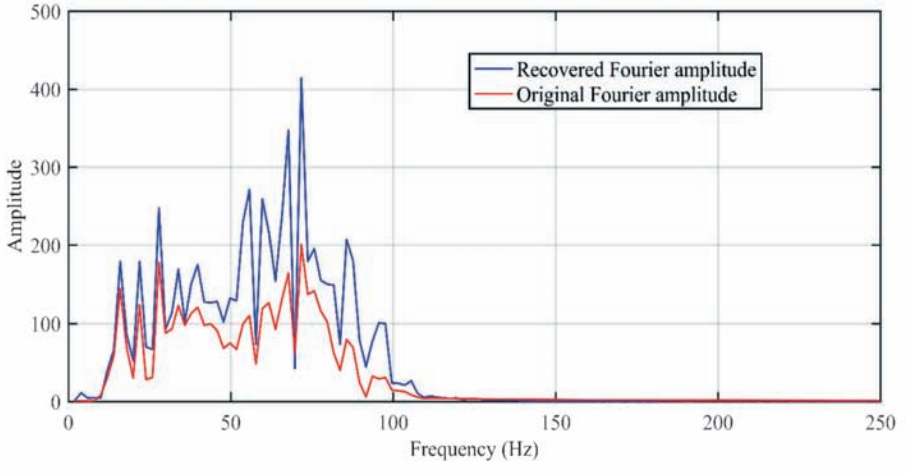

Fig. 9. The average Fourier spectrum comparison of the 100th, 150th and 200th seismic trace of Fig. 8. The red line is original real seismic data. The blue line is recovered seismic data from our proposed work flow.

REFERENCES

Aki, K. and Richards, P.G., 2002. Quantitative Seismology, 2nd Ed.. W. H. Freeman, San Francisco.

van der Baan, M., 2012. Bandwidth enhancement: Inverse Q filtering or time-varying Wiener deconvolution? Geophysics, 77(4). 133

Boashash, B. and Mesbah, M., 2004. Signal enhancement by time-frequency peak filtering. IEEE Transact. Signal Process., 52: 929-937.

Braga, I.L.S. and Moraes, F.S., 2013. High-resolution gathers by inverse filtering in the wavelet domain. Geophysics, 78(2): V53-V62.

Cheng, M.M., Mitra, N.J., Huang, X., Torr, P.H. and Hu, S.M., 2015. Global contrast based salient region detection. IEEE Transact. Pattern Analys. Mach. Intellig., 37: 569-582.

Candès, E.J. and Plan, Y., 2010. Matrix completion with noise. Proc. IEEE, 98: 925-936.
Cheng, J., Chen, K. and Sacchi, M.D., 2015. Robust principal component analysis for seismic data denoising. Abstr., GeoConvention RPCA 2015.
Daubechies, I., Lu, J. and Wu, H.T., 2009. Synchrosqueezed wavelet transforms: a tool for empirical mode decomposition. Mathematics, arXiv: 0912.2437.
Daubechies, I., Lu, J. and Wu, H.T., 2011. Synchrosqueezed wavelet transforms: An empirical mode decomposition-like tool. Appl. Computat. Harmon. Analys, 30: 243-261.
Gao, J., Yang, S., Wang, D. and Wu, R., 2011. Estimation of quality factor Q from the instantaneous frequency at the envelope peak of a seismic signal. J. Computat. Acoust., 19: 155-179.
Hargreaves, N.D., 2012. Inverse Q filtering by Fourier transform. Geophysics; 56(4): 519.
Kolsky, H.L., 1956. The propagation of stress pulses in viscoelastic solids. Philosoph. Magaz., 1(8): 693-710.
Lupinacci, W.M., de Franco, A.P., Oliveira, S.A.M. and de Moraes, F., 2016. A combined time-frequency filtering strategy for Q-factor compensation of poststack seismic data. Geophysics, 82(1): V1-V6.
Nazari Siahsar, M.A., Gholtashi, S., Kahoo, A.R., Marvi, H. and Ahmadifard, A., 2016. Sparse time-frequency representation for seismic noise reduction using low-rank and sparse decomposition. Geophysics, 81(2): V117-V24.
Quan, Y. and Harris, J.M., 1997. Seismic attenuation tomography using the frequency shift method. Geophysics, 62: 895-905.
Reine, C., Clark, R. and van der Baan, M., 2012. Robust prestack Q-determination using surface seismic data: Part 1. Method and synthetic examples. Geophysics.
Ricker, N., 1953. The form and laws of propagation of seismic wavelets. Geophysics, 18: 10-40.
Rosa, A.L.R., 1991. Processing via spectral modeling. Geophysics, 56: 1244-1251.
Tary, J.B., van der Baan, M., Herrera, R.H., 2016. Applications of high-resolution time-frequency transforms to attenuation estimation. Geophysics, 82(1): V7-V20.
Thakur, G., Brevdo, E., Fukar, N.S. and Wu, H.T., 2013. The synchrosqueezing algorithm for time-varying spectral analysis: Robustness properties and new paleoclimate applications. Signal Process., 93:1079-1094.
Tonn, R., 1991. The determination of the seismic quality factor Q from VSP data. A comparison of different computational methods. Geophys. Prosp., 39: 127.
Trickett, S., 2008. F-xy cadzow noise suppression. Expanded Abstr., 78th Ann. Internat. SEG Mtg., Las Vegas: 2586-2590.
Wang, P., Gao, J. and Wang, Z., 2014. Time-frequency analysis of seismic data using synchrosqueezing transform. IEEE Geosci. Remote Sens. Lett., 11: 2042-2044.
Wang, Y., 2002. A stable and efficient approach of inverse Q filtering. Geophysics, 67: 657-663.
Wang, Y., 2004. Q analysis on reflection seismic data. Geophys. Res. Lett., 31: 159-158.
Wang, Y., 2006. Inverse Q-filter for seismic resolution enhancement. Geophysics, 71(3): V51.
Wang, Y., 2009. Seismic Inverse Q filtering. John Wiley & Sons., New York.
Yang, Y., Ma, J. and Osher, S., 2013. Seismic data reconstruction via matrix completion. Inver. Probl. Imag., 7: 1379-1392.
Yilmaz, O., 2001. Seismic Data Analysis. Vol. 1. SEG, Tulsa, OK.
Zhang, C. and Ulrych, T.J., 2002. Estimation of quality factors from CMP records. Geophysics, 67: 1542-1547.
Zhou, H., Tian, Y. and Ye, Y., 2014. Dynamic deconvolution of seismic data based on generalized S-transform. J. Appl. Geophys., 108(9): 1-11.
Zhou, T. and Tao, D., 2011. Godec: Randomized Low-rank & Sparse Matrix Decomposition in Noisy Case. Internat. Conf. Mach. Learn. Omnipress, Washington D.C.